LUMINESCENCE QUANTUM EFFICIENCY AND LOCAL OPTICAL DENSITY OF STATES IN THIN FILM RUBY MADE BY ION IMPLANTATION

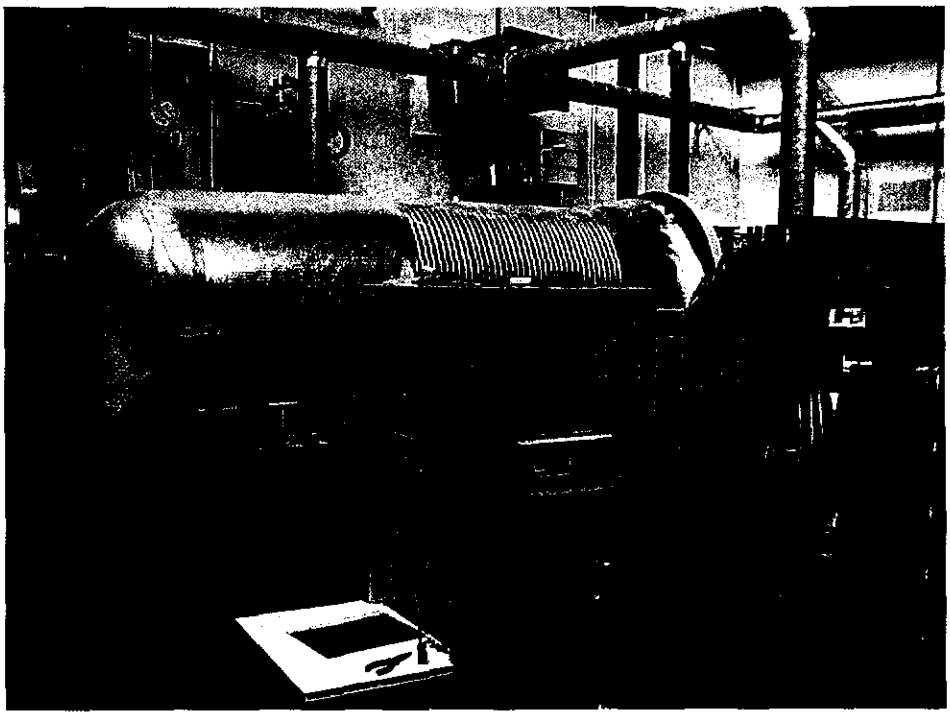

Verslag van het Groot Onderzoek voor de studie Experimentele Natuurkunde
aan de Universiteit Utrecht, maart 1999-april 2000

Michael Hensen
FOM-instituut voor Atoom- en Molecuulfysica
Kruislaan 407
1098 SJ Amsterdam

begeleiding:
drs M.J.A. de Dood
Prof. Dr. A. Polman

supervisor UU:
Prof. Dr. A. Polman

CONTENTS

ABSTRACT

Single crystal, <0001> oriented, sapphire samples were implanted with 150 keV Cr ions and characterized by Rutherford backscattering spectrometry (RBS) and photoluminescence (PL) measurements. The lifetime of the R lines around 694 nm was studied as function of Cr concentration. The implanted samples were covered with a range of transparent liquids. The decay rate of the Cr ions shows a clear dependence on the refractive index of the liquid. This effect is understood by a calculation of the optical density of states. By comparing the measured with calculated decay rates a radiative decay rate of 157 s^{-1} is found (QE=50 %).

INTRODUCTION

Spontaneous emission of atoms can be influenced by placing the atoms close to a dielectric interface within wavelength scale, as was first pointed out by Purcell [1]. We have studied the relative simple case of a planar interface between two dielectrics where Cr ions were incorporated close to the interface of a Al_2O_3 sample. The observed changes in spontaneous emission rate can be calculated by Fermi's Golden Rule using vacuum field fluctuations. These field fluctuations can be calculated for simple geometries and be described using a classical local density of states (LDOS) [2-5]. Experimentally the change in spontaneous emission rate was studied for example for atoms close to dielectric interfaces and mirrors [5-7], for atoms in the proximity of a glass substrate [8] and for recombination of electron-hole pairs in a slab bounded by two dielectrics [9]. Once characterized these samples can be used as probes of the LDOS in photonic crystals and absorbing systems.

Ion implantation is a simple technique to introduce Cr ions in the near surface of Al_2O_3. In the past much work has been done on the implantation of Cr ions to study surface hardening of Al_2O_3 [10-12]. However these ion-implanted samples were never characterized by luminescence measurements. Luminescence of Cr ions close to a dielectric interface was studied in thin film ruby lasers formed by epitaxial growth that were used as stress sensors [13,14]. In this case no attention was paid to luminescent lifetimes.

The optical properties of transition metal ions in solids have been studied for many years. Because these transition metals occur in the outer lying 3d electronic levels of the ion, a strong coupling between these levels and the local crystal field of the surrounding atoms in the solid exists. Especially Cr^{3+} ions in Al_2O_3 (ruby) have been studied intensively since the introduction of the ruby laser [15,16]. The energy levels are well understood in terms of ligand field theory [17-20]. The characteristic R lines in the red end of the visible spectrum (692.9 and 694.3 nm) occur due to a transition from the first excited ^2E state to the $^4A_2$ ground state. Because of the importance of this transition in ruby lasers there is a large amount of published work on R line luminescence. One of the quantities that has received much attention in literature is the fluorescent lifetime of the R lines and its temperature dependence. The lifetime was found to drop from 4 ms at 77 K to 3 ms at 300 K [21-24]. Besides as a laser, ruby has an application as high-pressure sensors. Here the pressure-induced frequency shift of the R lines, caused by a change in the local crystal field, is used for pressure determination [25-28].

The aim of this paper is to determine the radiative lifetime and quantum efficiency of the R line luminescence for ion implanted samples. This was done by comparing calculations of the local density of states (LDOS) with measured lifetimes of samples brought in contact with liquids with different refractive indices.

EXPERIMENTAL

1 mm thick <0001> oriented Al_2O_3 single crystals with low Cr content (<1 ppb), were implanted at room temperature with 150 keV Cr^+ ions. The current on the sample during implantation was kept below 0.1 $\mu A/cm^2$. The samples were rotated 7° with respect to the incoming Cr ion beam to avoid channeling in the [0001] crystal direction. After annealing, the samples were annealed for two hours at 1450°C. One sample implanted with 3.0 $x10^{15}$ Cr/cm^2 received a 1200°C anneal before the 1450°C anneal to study the annealing behavior of the samples.

Rutherford backscattering spectrometry (RBS) in combination with ion channeling was used to study the crystal structure before and after annealing as well as the chromium depth distributions. A 2.0 MeV $^4He^+$ beam was used at a scattering angle of 165°. The implanted doses were 0.6, 1.6, 2.5, 3.0 and $4.0x10^{15}$ Cr/cm^2, corresponding to peak concentrations of 0.04, 0.11, 0.18, 0.21 and 0.28 at% (assuming a density of $1.17x10^{23}$ $atoms/cm^3$ for Al_2O_3).

Photoluminescence (PL) measurements were performed at room temperature, using the 457.9 nm line of an Ar-ion laser as a pump source. Typical pump powers of 15 mW in a 0.3 mm diameter spot were used. The luminescence signal was detected using a 48-cm monochromator and a thermo-electrically cooled GaAs photomultiplier tube. The spectral resolution was 0.16 nm. The pump beam was chopped at 13 Hz using an acousto-optic modulator and the signal was collected using a lock-in amplifier. Decay traces were recorded with a spectral resolution of 0.40 nm and a time resolution of 400 ns using the GaAs photomultiplier tube in combination with a multichannel photon counting system.

RESULTS AND DISCUSSION

Fig. 1 shows RBS channeling measurements of Al_2O_3 samples implanted with $3.0x10^{15}$ Cr/cm^2 before and after annealing. The dotted line shows a channeling spectrum of the as implanted state. The channeling spectrum after annealing at 1200°C for one hour is shown by the dashed line. Annealing at 1450°C for one hour resulted in a good channeling spectrum (solid line), which is compared with the random spectrum of the sample annealed at the same temperature (dots). The yield of the random and channeling spectra at energies above 1.22 MeV was multiplied by a factor 50 for the sample annealed at 1450°C.

Comparing the random spectrum with the channeling spectrum of the as-implanted sample shows that the implantation causes a disordered region, but has not completely amorphised the Al_2O_3. The near surface region is relatively damage free. The depth at which the damage is at a maximum in the Al sublattice is about 100 nm. Although clear channeling is observed in the Al sublattice, no channeling is observed in the O sublattice. This means that the O sublattice, contrary to the Al sublattice, has been amorphized by the ion implantation as has been observed before [10-12]. Figure 1 shows that annealing at 1200°C for one hour removes part of the damage made by the implantation (in both the Al and O sublattices). After subsequent annealing at 1450°C the yield is almost as that of an unimplanted sample (not shown), indicating good crystal quality.

The random spectrum shows the implanted Cr distribution in the Al_2O_3. The Cr depth distribution could be fitted using a gaussian profile, peaking at 70 nm and with a full width at half-maximum (FWHM) of 115 nm. Because Cr is known to begin diffusing at a temperature of about 1600°C [10,11], we assume that the Cr distribution is the same for all the samples after annealing up to 1450°C. The small peak at the high energy side of the Cr peak is possibly due to a small amount of Fe (surface energy 1.51 MeV) at the surface or coimplanted with Cr.

The Cr section of the spectra in fig. 1 show that after annealing at 1450°C the minimum yield of the Cr ions almost vanishes (except at the sides of the Cr profile), indicating that the Cr ions are substitutional. Our results indicate that at least 95 % of the Cr ions are substitutional in agreement with literature. [10,11] To summarize the RBS results the first two columns of table 1 gives the minimum yield of the Al sublattice and of the integrated Cr distribution.

Figure 2 shows PL spectra at room temperature of Al_2O_3 implanted with $3.0x10^{15}$ Cr/cm^2 measured after implantation and after annealing at 1200°C and 1450°C. All spectra show two distinct peaks at energies of 14,403 and 14,432 cm^{-1} (corresponding to wavelengths at 694.3 and 692.9 nm respectively); often identified as the R lines. The lines can be very well fitted with Lorentzian line shapes [29]. For the sample that was annealed at 1200°C the FWHM is 15.2 cm^{-1} for the low energy peak (R_1 line) and 11.4 cm^{-1} for the high energy peak (R_2 line). After annealing at 1450°C, the FWHM reduces to 12.7 and 9.72 cm^{-1} (corresponding to 0.61 and 0.47 nm).

The R_1 and R_2 lines at 692.9 and 694.3 nm are characteristic for Cr^{3+} ions that are substitutional in the Al sublattice. The 457.9 nm line of the pump source is absorbed in the $^4T_1$ and $^4T_2$ broad bands [21]. Subsequently, rapid non-radiative relaxation to the first excited state ^2E occurs, followed by a radiative transition to the ground state $^4A_2$ [15,16,21]. The broadening of the R lines is caused by the Cr-lattice interaction. The FWHM measured in fig. 2 is somewhat larger than that measured for bulk Al_2O_3:Cr. A possible explanation for this could be that the Al_2O_3 lattice contains residual damage from the ion implantation that was not annealed completely [11].

From fig. 2 it is clear that the PL intensity increases with increasing anneal temperature. Although hard to identify in the figure the as-implanted sample shows two clear R lines, superimposed on a broad background. This is consistent with channeling measurements [11], that show evidence for a small Cr substitutional fraction after implantation. Annealing at 1200°C enhances the intensity by a factor 12; subsequent annealing at 1450°C yields a factor 45 higher intensity than the as-implanted sample. The increase in intensity could be explained by an increase in concentration of substitutional Cr and an increase in luminescence quantum efficiency. To study the last parameter, luminescence lifetime measurements were performed at 694.3 nm. The lifetimes are 2.02, 2.77 and 3.30 ms for the as-implanted and 1200°C / 1450°C annealed samples respectively. The measured lifetime increase of a factor 1.6 implies that the factor 45 intensity increase is due to an increase in the concentration of substitutional Cr after annealing.

Due to additional non-radiative processes the measured lifetime will be shorter than the radiative lifetime. It is known that ion implantation introduces defects and lattice strain in the crystal [11] that might not be completely removed by thermal annealing, leading to line broadening and non-radiative decay channels. This line broadening is observed in Fig. 1 and was discussed above. The total decay rate can be written as the sum of radiative and non radiative decay:

$$W = W_r + W_{nr} \tag{1}$$

Besides the R lines the emission spectrum shows broad bands and some small other lines. Figure 3 shows the PL spectrum for a sample implanted with 3.0×10^{15} Cr/cm^2, corresponding to 3.9 wt% Cr_2O_3. The sample was annealed one hour at 1200°C and one hour at 1450°C. The spectrum is normalized to the peak intensity of the R_1 line. The spectrum shows broad bands and some small lines at the low energy side of the R lines. The radiative lifetime τ_r ($=1/W_r$) of the R lines is found by integrating over all possible transitions. These also include processes that involve the creation or destruction of one or more phonons (phonon assisted decay) and transitions that are in thermal equilibrium with the R lines. Because the R_1 and R_2 lines are also in thermal equilibrium with each other they are expected to have the same lifetime as was indeed confirmed by temperature dependent measurements. The broad bands (vibronic sidebands) at the low energy side of the R lines are the result of phonon assisted decay and the small lines around 14,300 cm^{-1} are caused by the interaction between Cr ions (second and fourth nearest neighbors) [23,30]. The relative intensity of the N_1 line at 704.1 nm (second nearest neighbors) to the intensity of the R lines and vibronic sidebands is about 1 %, in agreement with measurements done in literature [23].

In order to study the luminescence quantum efficiency of the Cr ion PL decay measurements were performed in air and in case a liquid is brought in contact with the sample. The liquid is put between the implanted side of the sample and a microscope glass. The measurements were done at λ = 694 nm for a Al_2O_3 sample implanted with 3.0×10^{15} Cr/cm^2 annealed at 1450 °C. Two decay traces are shown in Fig. 3, that are both single exponential. The one measured in air gives a lifetime of 3.34 ms. The curve measured for n = 1.57 (2-methoxy-4 propenylphenol) shows a lifetime of 3.18 ms.

Fig. 4 shows the result of decay measurements that were performed for different refractive indices. Decay traces were measured in air and for n = 1.57 for samples implanted with 0.6, 1.6, 2.5, 3.0 and 4.0×10^{15} Cr/cm^2 that were annealed at 1450 °C. Furthermore the traces were measured for n = 1.33 (water) for all these samples. Decay traces for the samples implanted with 3.0×10^{15} Cr/cm^2 were also measured for n = 1.45 and 1.52. The measured data have error bars of 3 s^{-1}. Fig. 4 shows that the dependence of the decay rate on refractive index is linear and that the decay rate increases for increasing concentration.

A description of the fluid experiments in terms of a LDOS makes it possible to extract from the measured data the luminescence quantum efficiency. The spontaneous emission rate can be calculated using Fermi's Golden Rule [4,5]. Using the field operator consisting of creation and annihilation operators the i-th cartesian component of the spontaneous emission rate is given by [5]:

$$W_i(\mathbf{R}) = \frac{\pi\omega}{\hbar\varepsilon(\mathbf{R})}|\mathbf{D}_{ab}|^2 \cdot \rho_i(\omega,\mathbf{R}) \tag{2}$$

D_{ab} is the dipole matrix element of the atomic transition between an excited energy state b and the ground state a of the atom. The energy states b and a are separated by energy• ω. ρ_i is the i-th cartesian component of a local density of states (LDOS). ρ_i can be calculated classically by solving the classical Maxwell equation for a system with a dielectric interface between Al_2O_3 and a dielectric with refractive index n. It is also possible to find an expression for the spontaneous emission rate in terms of zero-point field fluctuations for the system [3,4]. The total emission rate W_{tot} is expressed in terms of a local density of states (LDOS) $f_{1.76}$, that is normalized to 1 for bulk Al_2O_3 with refractive index 1.76:

$$W_{tot}(n) = W_{nr} + f_{1.76}(n) \cdot W_r^{1.76} \tag{3}$$

Fig. 5 shows calculations of $f_{1.76}$ as a function of the distance from the dielectric interface z. The dashed line is the result of a calculation (based on field fluctuations [4]) for a system of an infinite half space of Al_2O_3 and an infinite half space of air (n=1.00). The solid line shows the calculation for Al_2O_3 in contact with a medium with a refractive index of 1.57. The position of the peak of the Cr distribution is indicated by the arrow. Fig. 5 shows that the radiative decay rate is suppressed towards the interface and increases for increasing refractive index. This last observation is supported by the data from Fig. 4.

In order to calculate the effect of the variation in LDOS on the Cr decay rate, the curves in Fig. 5 were integrated over the Cr depth distribution as determined by RBS (see Fig. 1). Such calculations were done for refractive indices of 1.0, 1.15, 1.3, 1.45 and 1.76. The result of this calculations is shown by the dotted line in fig. 4 for the case W_{nr} = 0. Note that this LDOS calculation only yields the relation variation of W_r with n. In the calculation the bulk value of W_r was taken 320 s^{-1} in order to have a clear overview of the situation in one figure.

The relation variation of the decay rate with n of Fig. 4 shows that the radiative decay rate is the same for all concentrations. The solid lines are fits to the data assuming similar radiative rates for all concentrations, but different non-radiative rates. Since the LDOS $f_{1.76}$ as function of refractive index is known and the total decay rate has been measured, it is possible to determine the radiative and non-radiative decay rate from equation (5) for the different samples. The result is 157 ± 10 s^{-1} for the radiative decay rate in bulk sapphire. The quantum efficiencies are 52, 51, 49, 49 and 47 % for the samples implanted with 0.6, 1.6, 2.5, 3.0 and 4.0×10^{15} Cr/cm^2 respectively.

Fig. 6 shows the PL decay rate as a function of Cr peak concentration, after annealing at 1450°C. The decay rate increases linearly with Cr concentration. The extrapolated PL decay rate for zero Cr concentration is 276 s^{-1}, corresponding to a lifetime of 3.15 ms in bulk sapphire. This value is much smaller than our experimental radiative lifetime of 6.4 ms. One possible explanation is non-radiative decay that is independent of Cr concentration. Another possibility is that for concentrations lower than we have measured the decay rate does not depend linearly on Cr concentration any more. This could be caused by a decreasing non-radiative decay rate for decreasing Cr concentration. Furthermore our experimental radiative lifetime is also larger than the value of 4 ms found by others [21,22]. This could be due to a local environment of the Cr in our samples that is different from the local environment of Cr in bulk sapphire. This observation is supported by the line broadening from Fig. 2.

Conclusion

This work shows it is possible to optically dope sapphire with Cr by ion implantation and afterwards thermal annealing. Implanted samples were characterized by RBS and PL measurements that show that after annealing at 1450°C more than 95 % of the Cr ions are substitutional. Lifetimes around 694 nm were measured as a function of refractive index of transparent liquids covering the sample. The lifetime clearly decreased with increasing refractive index. Emission rates were also calculated using field fluctuations and compared to the measured rates. This comparison resulted in values for the radiative lifetime and quantum efficiency.

The theory of field fluctuations gives a clear understanding of the dependency of the lifetime on refractive index for transparent liquids. We hope that this understanding will give us more insight in the situation of absorbing or strongly scattering media, where theory is less well developed.

REFERENCES

1 E. M. Purcell, Phys. Rev. **69**, 681 (1946)
2 H. Khosravi and R. Loudon, Proc. R. Soc. London A **433**, 337 (1991)
3 H. Khosravi, R. Loudon, Proc. R. Soc. Lond. A **436**, 373 (1992)
4 H. P. Urbach and G. L .J. A. Rikken, Phys. Rev. A **57**, 3913 (1997)
5 E. Snoeks, A. Lagendijk, and A. Polman, Phys. Rev. Let. **74**, 2459 (1994)
6 K. H. Drexhage, J. Lumin. **1,2**, 693 (1970)
7 W. L. Barnes, Journal of Modern Optics, **45**, 661-699 (1998)
8 W. Lukosz and R. E. Kunz, Optics Commun. **31**, 42 (1979)
9 E. Yablonovitch, T. J. Gmitter and R. Bhat, Phys. Rev. Lett. **61**, 2546 (1988)
10 G. C. Farlow, C. W. White, C. J. McHargue, and B. R. Appleton, Mat. Res. Symp. Proc. **27**, 395 (1984)
11 H. Naramoto, C. W. White, J. M. Williams, C. J. McHargue, O. W. Holland, M. M. Abraham, and B. R. Appleton, J. Appl. Phys. **54**, 683 (1982)
12 C. W. White, G. C. Farlow, C. J. McHargue, P. S. Sklad, and B. R. Appleton, Nuclear Instruments and Methods in Physics Research B **7/8**, 473 (1985)
13 Ning Yu, Qingzhe Wen and David R. Clarke, P. C. McIntyre, Harriet Kung, and M. Nastasi, T. W. Simpson and I. V. Mitchell, DeQuan Li, J. Appl. Phys. **78**, 5412 (1995)
14 Q. Wen and D. R. Clarke, Ning Yu and M. Nastasi, Appl. Phys. Lett. **66**, 293 (1995)
15 T. H. Maiman, Physical Review **123**, 1145 (1961)
16 T. H. Maiman, R. H. Hoskins, I . J. Haenens, C. K. Asawa, and V. Evtuhov, Physical Review **123**, 1151 (1961)
17 R. M. Macfarlane, J. Chem. Phys. **39**, 3118 (1963)
18 S. Sugano and M. Peter, Phys. Rev. **122**, 381 (1961)
19 R. M. Macfarlane, J. Chem. Phys. **39**, 3118 (1963)
20 S. Sugano, Y. Tanabe, and H. Kamimura, *Multiplets of Transition-Metal Ions in Crystals* (Academic, New York, 1970)
21 D. F. Nelson and M. D. Sturge, Physical Review **137,** A1117 (1964)
22 N. A. Tolstoi and L. Shun'-Fu, Optics and Spectroscopy **13**, 224 (1962)
23 G. F. Imbusch, Physical Review **153**, 326 (1966)
24 F. Versanyi, D. L. Wood, and A. L. Schawlow, Physical Review Letters **3**, 544 (1959)
25 J. H. Eggert, Kenneth A. Goettel, and I. F. Silvera, Physical Review B **40**, 5733 (1989)
26 Y. Sato-Sorensen, J. Appl. Phys. **60**, 2985 (1986)
27 J. H. Eggert, Kenneth A. Goettel, and I. F. Silvera, Physical Review B **40**, 5724 (1989)
28 W. L. Vos and J. A. Schouten, J. Appl. Phys. **69**, 6744 (1991)
29 D. E McCumber and M. D. Sturge, Journal of Applied Physics **34**, 1682 (1963)
30 G.F. Imbusch and R. Kopelman, *Topics in Applied Physics* **49**

	χ^{Al}(%)	χ^{Cr}(%)	I_{PL}(694.3 nm)	τ_{PL}(694.3 nm)
as-implanted	53	50	0.02	2.02
1200°C	13	70	0.26	2.77
1450°C	4	3	1.00	3.30

TABLE 1: Minimum yield in RBS channeling for the Al sub-lattice and the integrated Cr depth distribution, measured after different anneal treatments. The normalized PL intensities and lifetimes measured at 694.3 nm are also shown.

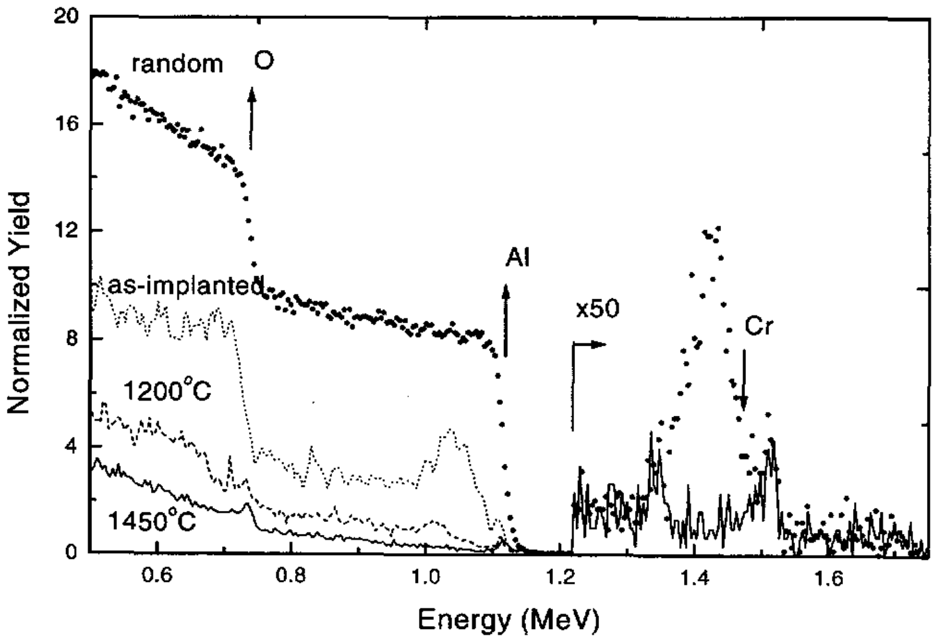

FIGURE 1: RBS spectra of Cr-implanted ($3.0x10^{15}$ Cr/cm^2) Al_2O_3. Channeling spectra are shown for the as-implanted sample and samples annealed at 1200°C and 1450°C. A random spectrum after 1450°C annealing is also shown. The Cr section in the spectrum is enlarged by a factor 50 and is only shown for the random and channeled spectrum of the sample annealed at 1450°C.

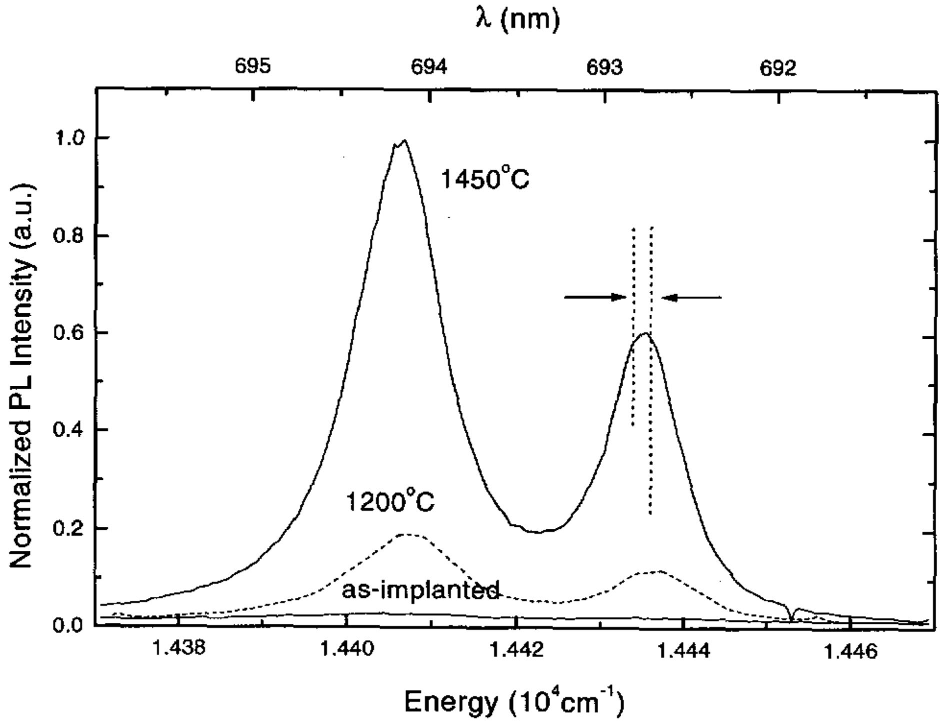

FIGURE 2: Room temperature PL spectra of Al_2O_3 implanted with 3.0×10^{15} Cr/cm^2. Data are shown for the as-implanted sample, after annealing for one hour at 1200°C and after an additional anneal for one hour at 1450°C. The peak wavelengths are 694.3 nm and 692.9 nm respectively. The peak FWHM is 12.7 and 9.72 cm^{-1} respectively, λ_{pump}=457.9 nm, power=15 mW.

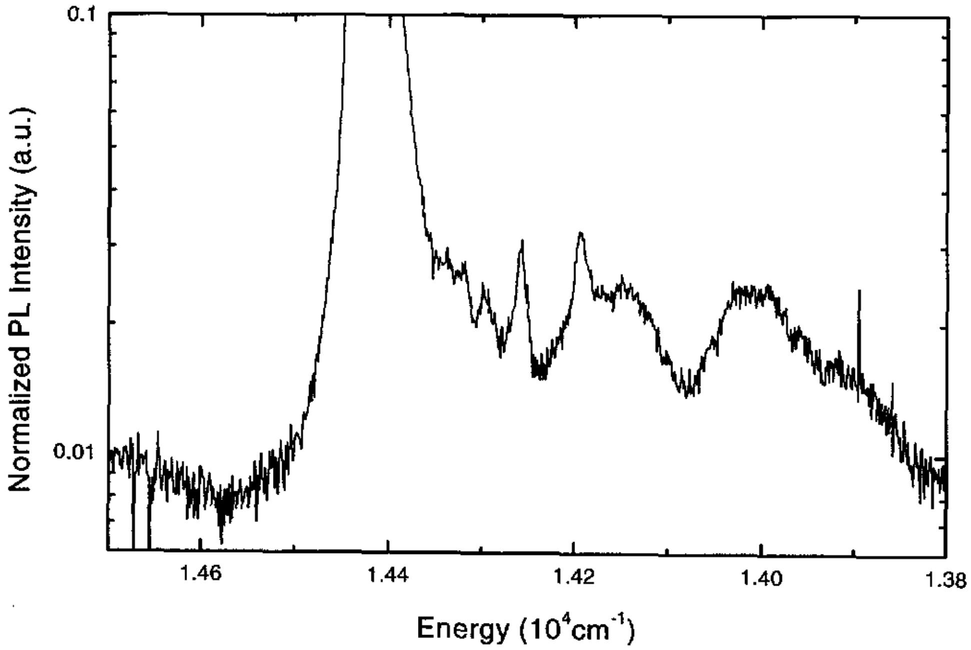

FIGURE 3: PL spectrum of Al_2O_3 implanted with $3.0x10^{15}$ Cr/cm^2 (annealed for one hour at 1200°C and for one hour at 1450°C). The lines around 14,400 cm^{-1} are the R lines with at their low energy side the vibronic side bands around 14,200 cm^{-1} and 14,000 cm^{-1} (these are two broad bands). The small lines around 14,200 cm^{-1} are caused by closely coupled pairs (second- and fourth nearest neighbor pairs) and are called the N lines.

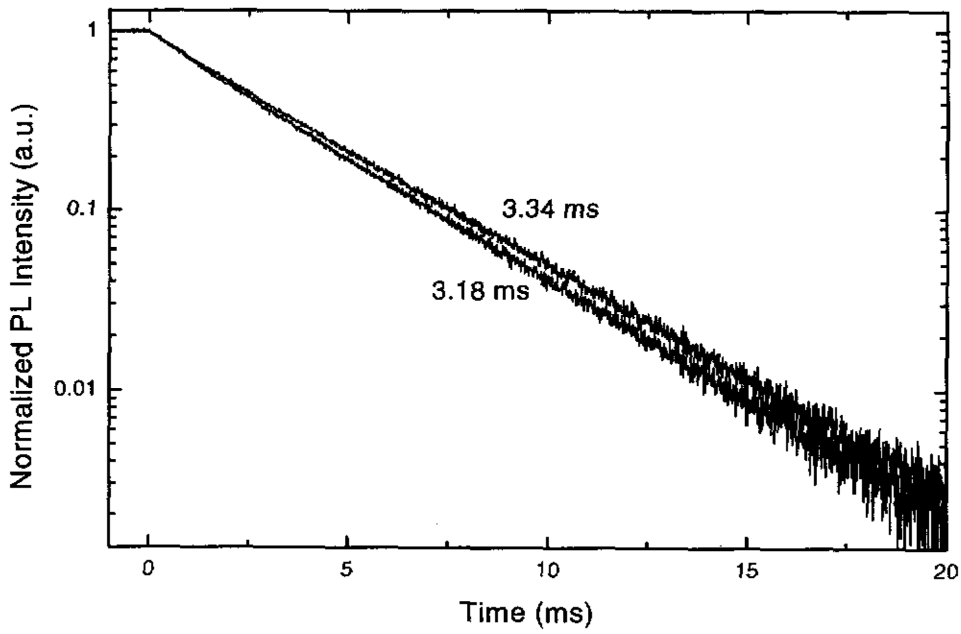

FIGURE 4: Decay traces for a Al_2O_3 sample implanted with $3.0x10^{15}$ Cr/cm^2 (annealed two hours at 1450°C). The curve with the longest lifetime (3.34 ms) was measured in air. The curve with the smallest lifetime (3.18 ms) was measured with a liquid with refractive index 1.57 brought in contact with the sample. The decay traces are nicely single exponential over at least three orders of magnitude.

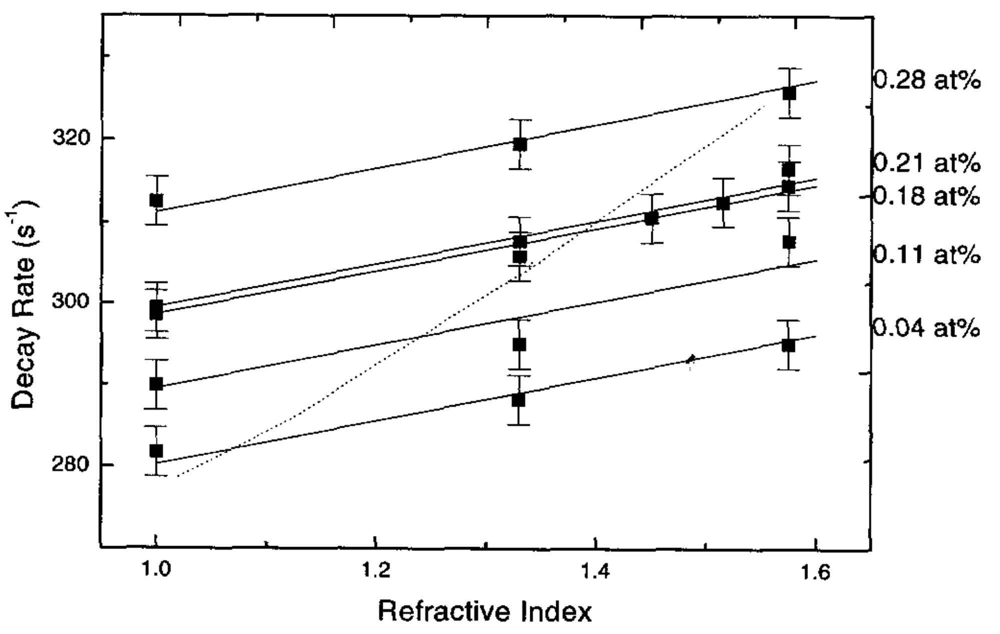

FIGURE 5: Measured decay rates at 694 nm (R lines) as a function of refractive index of covering liquids. Decay rates measured in air are also shown. Data are shown for Cr peak concentrations of 0.04, 0.11, 0.18, 0.21 and 0.28 at%, and all samples were annealed at 1450 C. A calculation of the dependence of the purely radiative rate on refractive index is shown by the dotted line. The drawn lines are fits to the data assuming similar radiative rate for all concentrations, but different non-radiative rates. The result for the radiative decay rate is $157.5 \pm 10\ s^{-1}$ (QE=50%). The dotted line is the calculated LDOS $f_{1.76}$ (normalized to 1.0 for bulk Al_2O_3). The LDOS is integrated over the Cr depth distribution that was obtained by the RBS measurement.

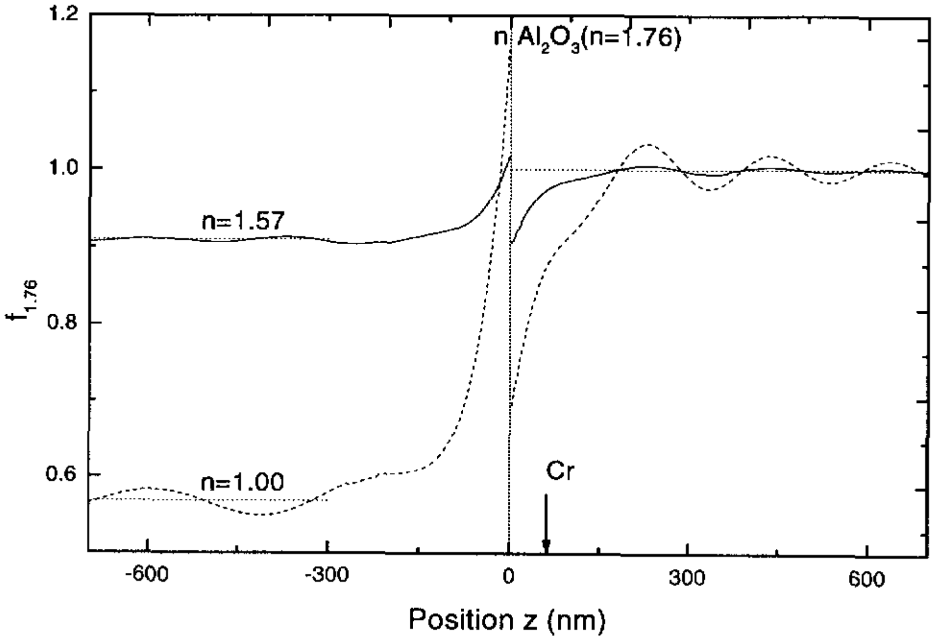

FIGURE 6: Local optical density of states (LDOS) $f_{1.76}$ calculated around the interface between Al_2O_3 and a liquid with refractive index n. The LDOS is normalized to the value in bulk sapphire. The solid line shows the result of the calculation for n=1.57 and the dotted line that for n=1.00. The position of the peak of the Cr distribution is indicated by the arrow.

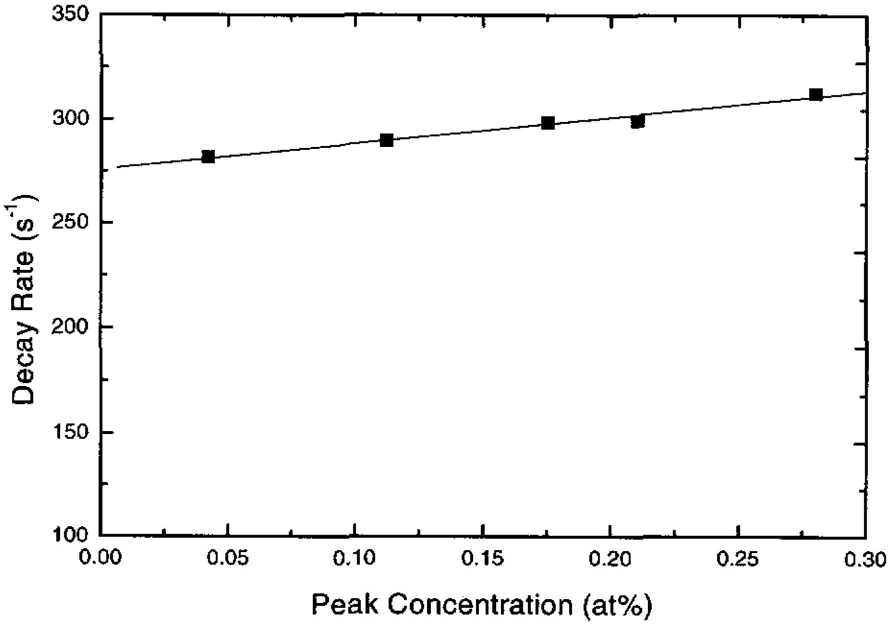

FIGURE 7: PL decay rate as a function of Cr peak concentration, after annealing at 1450°C. The solid line is a linear fit through the data. The extrapolated PL decay rate for zero Cr concentration is 276 s^{-1}.

Luminescence quantum efficiency in absorbing or strongly scattering systems

By comparing calculations of a local optical density of states (DOS) with measured lifetimes in transparent systems Al_2O_3 samples implanted with Cr^+ ions were characterized. These samples can be used as probes of the DOS in photonic crystals or absorbing systems, where theory is less well developed.

Lifetime measurements for strongly scattering systems

All lifetime measurements for strongly scattering systems were done with a Al_2O_3 sample implanted with $3.0x10^{15}$ Cr/cm^2 that was annealed at 1450°C. As a first try measurements were done with a solution of ZnS spheres with a diameter of 1 μm. The solution of ZnS spheres was put between the sample and a microscope glass and now and then a new drop of solution was added because the ethanol evaporated very quickly. The lifetime reduced from 3.32 ms in air to 3.17 ms for the solution of spheres. Fig. 5 shows the decay rate as a function of refractive index for transparent liquids. Ethanol has a refractive index of 1.36, which corresponds to a lifetime of 3.24 ms.

The lifetime was measured after the ethanol of a solution of ZnS spheres (diameter 1 μm) had evaporated. Now the lifetime reduced from 3.34 ms in air to 3.31 ms for the ZnS spheres. After twice repeating this evaporation procedure the lifetime reduced to 3.28 ms.

Lifetimes were also measured for SiO_2 colloids with a diameter of 1245 nm deposited on the sample. Colloids were taken from a sedimented ethanol suspension to have a high concentration. After evaporation of the ethanol the sample, that was put under an angle, was clearly covered with a layer of colloids that seemed to have a crystalline structure (for certain directions Bragg reflections could be seen). To see if there were crystalline regions the sample was looked at with an optical microscope with magnification of 100. Fig. 8 shows a part of the sample (56.4 x 43.4 μm^2) that shows relatively much crystalline regions. The lifetime was measured for four different positions of the spot on the sample of the pump beam. A reduction of the lifetime of 3.34 ms in air to 3.28 (average of the four measurements) ms for the colloids could be seen.

Lifetime measurements for absorbing systems

As a first absorbing system we used a solution of the laser dye HITCI (molecular weight 536.5) in methanol (methanol has a refractive index of 1.33). HITCI shows strong absorbance for wavelengths from 600 to 800 nm. HITCI was solved to a concentration of 0.0186 Ml^{-1} (the maximum solubility of HITCI was indeed given by about 10 gl^{-1}). The sample we used was implanted with $0.6x10^{15}$ Cr/cm^2 and annealed at 1450°C. To do lifetime measurements the sample was glued on a cuvet with a small hole in it (because HITCI is known to be toxic). The lifetime reduced from 3.54 ms in air to 3.48 ms in methanol. Bringing the solution of HITCI in methanol in the cuvet gave a lifetime of 3.47 ms.

To raise the concentration of laser dye on the sample a layer of HITCI solved in PMMA (poly methyl meta aerylaat) was spin coated on the sample ($0.6x10^{15}$ Cr/cm^2; annealed at 1450°C). The sample was spin coated at 2000 rpm for 30 s and after that heated for one hour at 200°C. These spin coat conditions are known to give a layer on the sample of a thickness of about 500 nm. The spin coated sample looked a little green but was almost transparent. Decay measurements gave a lifetime of 3.58 ms in air and a lifetime of 3.45 ms for the spin coated sample.

To further investigate the lifetime for absorbing systems a sample of silicon that was brought as close as possible to a Al_2O_3 sample implanted with $3.0x10^{15}$ Cr/cm^2 and annealed at 1450°C. A microscope picture showed that the distance between the two samples was about 50 μm. The lifetime showed a reduction of 3.28 ms in air to 3.25 ms for the silicon.

As a last absorbing system a solution of Fe_3O_4 spheres with a diameter of 10 nm in decaline (decahydronaftaleen) was taken of a concentration of about 500 gl^{-1}. The solution was put between a microscope glass and the sample ($3.0x10^{15}$ Cr/cm^2; annealed at 1450°C). The refractive index of Fe_3O_4 is 2.4;the refractive index of the solvent decaline 1.58, corresponding to a lifetime of 3.05 ms). The lifetime for the case that the solution of the colloids was brought in contact with the sample was 3.05 ms.

FIGURE 8: A part of the sample (56.4x43.4 μm^2) where there are relatively much crystalline regions.

LUMINESCENCE AND RADIATIVE LIFETIME OF CR^{3+} IONS IN AL_2O_3

Luminescence of Cr^{3+} ions takes place due to electronic transitions of the 3^d electrons. Because these electrons are not shielded, the sapphire crystal splits up the energy levels of a Cr^{3+} ion in vacuum. In Al_2O_3 doped with Cr^{3+} ions (ruby) the chromium ion has a well-defined position in the crystal, leading to well defined energy levels, given in Fig. 9. The Cr^{3+} ions are excited in the broad $^4T_1$ band, using the 457.9 nm line of an Ar ion laser. Then there is a quick decay between the $^4T_1$ band and the ^2E state. The decay from the split ^2E state to the $^4A_2$ ground causes the characteristic R-lines in the luminescence spectrum at a wavelength of about 694 nm. The decay rate of an i^{th} excited energy level to the ground state by emission of a photon is defined by W^i_R(R-line). The emission of the photon from an i^{th} excited energy level by the creation or destruction of one or more phonons the decay rate gives rise to vibronic sidebands with a rate W^i_R(vib). These vibronic sidebands give relatively broad luminescence. The total decay rate from radiative processes W^i_R is given by the sum of the decay rates from the sharp line (no-phonon line) and vibronic sidebands. Additional non-radiative decay is given by W^i_{NR}.

The fluorescence intensity of an excited energy state i as function of frequency and temperature is given by:

$$I^i(\nu,T) = CN^i\sigma^i_e(\nu,T)W^i_R \tag{1}$$

N^i is the number of atoms in the i^{th} energy level, C is a constant, $\sigma^i_e(\nu,T)$ is the emission cross section.

Looking at the ratio η^i (defined as the radiative efficiency) of the intensity integrated over the no-phonon line to the total integrated intensity, we obtain the relation:

$$\frac{\int\limits_{\substack{no-phonon\\line}} d\nu I^i(\nu,T)}{\int\limits_{\substack{total\\spectrum}} d\nu I^i(\nu,T)} = \frac{\int\limits_{\substack{no-phonon\\line}} d\nu\sigma^i_e(\nu,T)}{\int\limits_{\substack{total\\spectrum}} d\nu\sigma^i_e(\nu,T)} = \frac{W^i_R(no-phonon-line)}{W^i_R} = \eta^i \tag{2}$$

Here the following relation is used [21]:

$$W^i_R(R-line) = \frac{(\omega_i\mu_i)^2}{(2\pi c)^2}\exp[\hbar(\mu-\omega_i)/kT]\int\limits_{4\pi} d\Omega\int\limits_{i}\sigma^i_e(\omega)\frac{d\omega}{2\pi} \tag{3}$$

where μ_r is the refractive index of the bulk crystal; the emission cross section is integrated over the i^{th} line.

By relation (2) it follows we have to multiply (3) by $(\eta^i)^{-1}$ to obtain the emission rate due to all radiative processes. After summation over i and k and integration over solid angle Ω, the following relation for the lifetime due to all radiative processes is obtained:

$$W = 4\pi c e^{\hbar\mu/kT}\sum_i(\nu_i\mu_r)^2 e^{-2\pi\hbar c/kT}\int\limits_i[\tfrac{4}{3}(\frac{\sigma_\perp}{\eta_\perp})+\tfrac{2}{3}(\frac{\sigma_{//}}{\eta_{//}})]d\nu \tag{4}$$

The absorption cross section and radiative efficiency are given by a perpendicular and parallel part.

We cannot use (4), because we cannot distinguish experimentally between the vibronic sidebands of the R-lines and the emission of the excited levels other than the ^2E state and their phonon-assisted emission. From the definition of the radiative efficiency, the vibronic sideband of the R-line includes all the other no-phonon lines and their phonon-assisted emission. This part of the sum in (4) is therefore included in the term of the R-lines and we have finally:

$$W = 16\pi c\mu_r^2 \left\{ \sum_{i=1,2} v_i^2 e^{-2\pi\hbar cv/kT} \int_i [\tfrac{2}{3}(\frac{\sigma_\perp}{\eta_\perp}) + \tfrac{1}{3}(\frac{\sigma_{//}}{\eta_{//}})] dv \Big/ \sum_{i=1}^{5} e^{-2\pi\hbar hv/kT} \right\} \tag{5}$$

When the absorption cross sections for the R lines in ruby are determined, it is not difficult to calculate the radiative lifetime. The calculated lifetimes can be compared with the measured lifetimes; the difference between calculation and measurement is probably caused by non-radiative decay. In our experiment the intensity of the excited Cr^{3+} ions was measured, so this makes the calculation more complex. It is possible to relate the lifetime to an intensity spectrum, by using the relation between the absorption cross section and the intensity, given by (1). Equation (4) for the radiative lifetime can now be expressed in terms of the intensity spectrum. Solving the rate equations for a simple three level system we find the value for N (N is the number of particles in both the R_1 and R_2 energy levels): N=C/W. W is the total decay rate and C is a constant. Equation (1) for i=1,2 (R_1 and R_2) gives:

$$\begin{aligned} I^1(v,T) &= \frac{C\sigma_e^1(v,T)W_R^1}{W(e^{-\Delta/kT}+1)} \\ I^2(v,T) &= \frac{C\sigma_e^2(v,T)W_R^2}{W(e^{\Delta/kT}+1)} \end{aligned} \tag{6}$$

C is a constant and Δ is the energy difference between the ^2E levels. Equation (5) in terms of intensity becomes:

$$W = \frac{C\sqrt{16\pi c\mu_r^2}}{\sum_{i=1}^{5} e^{-2\pi\hbar cv_i/kT}} \left\{ v_1 e^{-2\pi\hbar cv_1/kT} \sqrt{\int_{R_1} \frac{I^1(v_1,T)(e^{-\Delta/kT}+1)}{\eta} dv_1} + v_2 e^{-2\pi\hbar cv_2/kT} \sqrt{\int_{R_2} \frac{I^2(v_2,T)(e^{\Delta/kT}+1)}{\eta} dv_2} \right\} \tag{7}$$

Using the measured intensity spectra for different temperatures, the lifetime due to all radiative processes can be calculated. The only parameter that is unknown is the constant C. Fortunately, we know the radiative lifetime for room temperature from the fluid experiment. From this value the constant C can be determined. Table 2 gives the values of the integrated intensities and radiative efficiencies for the measured spectra.

Temperature [K]	Integrated intensity R_1 line [10^{-7}]	Integrated intensity R_2 line [10^{-7}]	Ratio of the integrated R_1 and R_2 lines to the total integrated intensity
60	1.10	0.31	0.48
100	1.04	0.37	0.57
140	1.18	0.48	0.61
180	1.35	0.62	0.63
220	1.79	0.82	0.67
260	2.34	1.05	0.69
300	2.91	1.29	0.70

Table 2 Integrated intensities of the R_1 and R_2 lines and the ratio of the integrated R_1 and R_2 intensity to the total integrated intensity

The calculations are simplified by dividing both the dominator and numerator of equation (7) by $e^{-2\pi c\hbar\nu_1/kT}$. This gives:

$$W = \frac{(1.56\times10^{-6})\sqrt{16\pi c\mu_r^2}}{1+\exp[\frac{2\pi\hbar c}{kT}(\nu_1-\nu_2)]+\exp[\frac{2\pi\hbar c}{kT}(\nu_1-\nu_3)]+\exp[\frac{2\pi\hbar c}{kT}(\nu_1-\nu_4)]+\exp[\frac{2\pi\hbar c}{kT}(\nu_1-\nu_5)]}\times \quad (8)$$

$$\left\{\nu_1\sqrt{\frac{\int_{R_1} I^1(\nu_1,T)(e^{-\Delta/kT}+1)}{\eta}d\nu_1}+\nu_2\exp[\frac{2\pi\hbar c}{kT}(\nu_1-\nu_2)]\sqrt{\frac{\int_{R_2} I^2(\nu_2,T)(e^{\Delta/kT}+1)}{\eta}d\nu_2}\right\}$$

Fig. 10 shows the decay rates, calculated from equation (8), for temperatures ranging from 60 to 300 K. Calculations done by others are also shown [21]. Besides calculated decay rates Fig. 10 shows measured decay rates for samples implanted with 0.6 and 3.0x10^{15} Cr/cm^2.

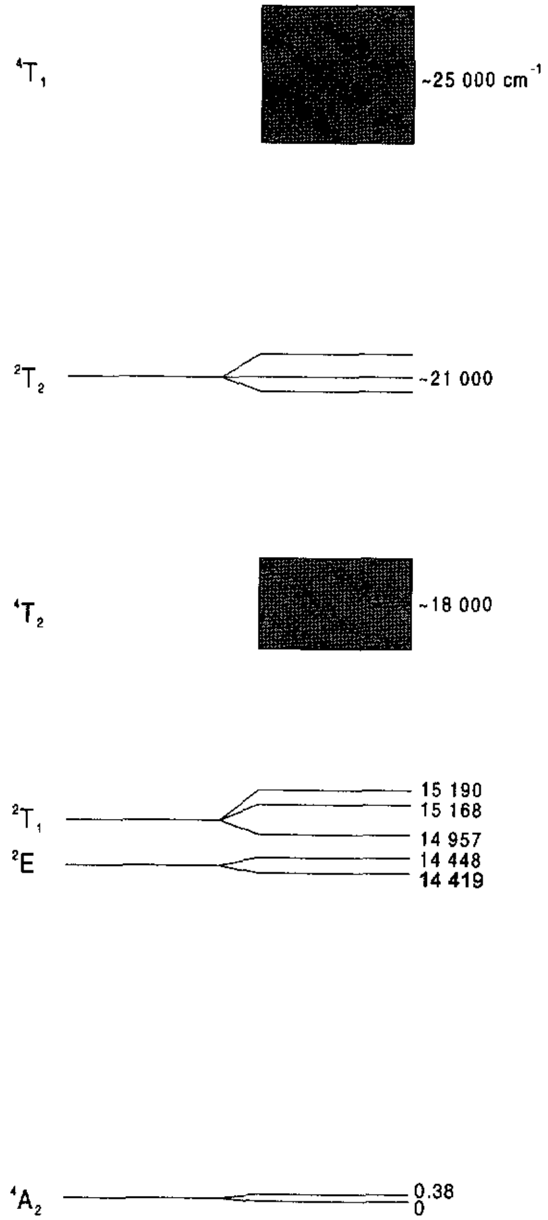

FIGURE 9: Energy levels of ruby

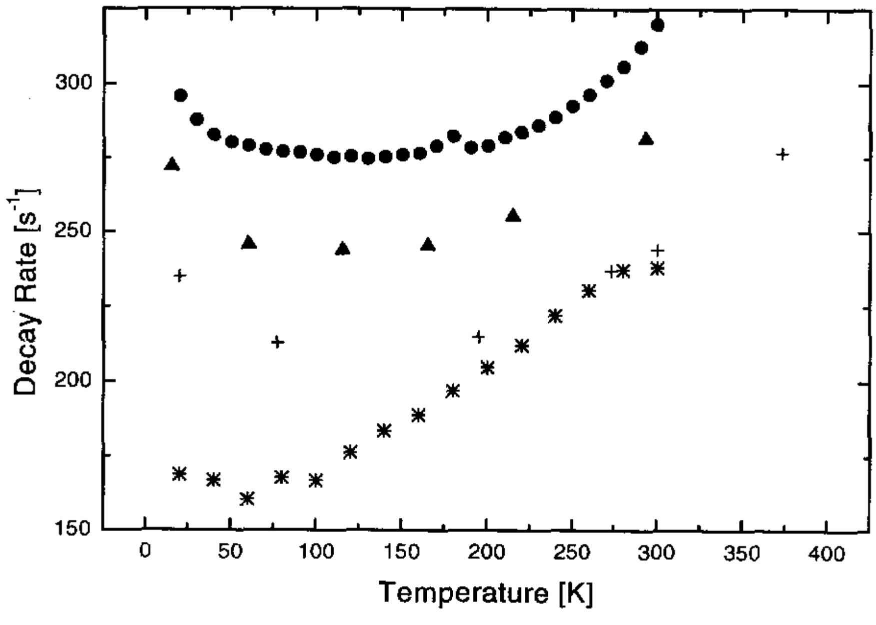

FIGURE 10: Decay rates measured for samples implanted with 0.6 and 3.0×10^{15} Cr/cm^2 (circles and triangles respectively) and calculated decay rates according to formula (8) (stars) and by [21] (crosses).